

# Comprehensive RNA Sequencing in Adenoma-Cancer Transition Identified Predictive Biomarkers and Therapeutic Targets of Human CRC

Mingzhe Zhu,<sup>1,2,5</sup> Yanqi Dang,<sup>1,5</sup> Zhenhua Yang,<sup>1,4</sup> Yang Liu,<sup>3</sup> Li Zhang,<sup>1</sup> Yangxian Xu,<sup>3</sup> Wenjun Zhou,<sup>1</sup> and Guang Ji<sup>1</sup>

<sup>1</sup>Institute of Digestive Diseases, Longhua Hospital, China-Canada Center of Research for Digestive Diseases (ccCRDD), Shanghai University of Traditional Chinese Medicine, Shanghai 200032, China; <sup>2</sup>School of Public Health, Shanghai University of Traditional Chinese Medicine, Shanghai 200032, China; <sup>3</sup>Department of General Surgery, Longhua Hospital, Shanghai University of Traditional Chinese Medicine, Shanghai 200032, China; <sup>4</sup>Digestive Endoscopy Department, Longhua Hospital Affiliated to Shanghai University of Traditional Chinese Medicine, Shanghai 200032, China

**Specific molecular biomarkers for predicting the transition from colorectal adenoma to cancer have been identified, however, circular RNA (circRNA)-related signatures remain to be clarified. We carried out high-throughput RNA sequencing to determine the expression profiles of circRNAs, microRNAs (miRNAs), and mRNAs in human colorectal cancer (CRC), adenoma, and adjacent normal tissues. We identified 84 circRNAs, 41 miRNAs, and 398 mRNAs that were commonly differentially expressed in CRC and adenoma tissues compared with normal tissues. Gene Ontology (GO), Kyoto Encyclopedia of Genes and Genomes (KEGG) pathway, and protein-protein interaction (PPI) analyses identified numerous cancer-related hub genes that might serve as potential therapeutic targets in CRC. Competing endogenous RNA (ceRNA) networks, including three circRNAs, three miRNAs, and 28 mRNAs were constructed, suggesting their potential role in cancer progression. Representative differentially expressed RNAs were validated by the Cancer Genome Atlas (TCGA) database and real-time PCR experiments. Receiver operating characteristic (ROC) curve analysis identified three circRNAs (*hsa\_circ\_0049487*, *hsa\_circ\_0066875*, and *hsa\_circ\_0007444*) as possible novel biomarkers predicting the transition from colonic adenoma to cancer. Overall, our findings may provide novel perspectives to clarify the mechanisms of the transition from premalignant adenoma to cancer and identify specific circRNA-related signatures with possible applications for the early diagnosis of and as potential therapeutic targets in CRC.**

## INTRODUCTION

Colorectal cancer (CRC) is the third most common cancer worldwide, with increasing incidence and mortality in China.<sup>1,2</sup> The transition from adenoma to carcinoma has been proposed as a critical step in colorectal carcinogenesis, including multiple genetic and epigenetic risk factors.<sup>3,4</sup> Up to 90% of CRC cases follow this transition over a period of many years,<sup>5</sup> offering opportunities for the early screening, prediction, and prevention of CRC.

Genetic and epigenetic alterations are critical in driving adenoma-carcinoma progression, and numerous molecular signatures have been identified. For example, *EZH2* and *COX-2* gene expression levels were increased in both colorectal adenoma and carcinoma compared with normal tissues, contributing to CRC progression and with potential uses in the early diagnosis of CRC.<sup>6,7</sup> Whole-genome expression profiling of colorectal adenoma and CRC samples revealed a set of downregulated transcripts (e.g., *MAL*, *SFRP1*, *SULT1A1*, etc.) along the adenoma-carcinoma transition.<sup>8</sup> Researchers also identified specific microRNA (miRNA) profiles in the adenoma-to-carcinoma progression using microarray analysis.<sup>9</sup>

Circular RNAs (circRNAs) are a novel class of endogenous noncoding RNAs that form covalently closed continuous loops without 3' end poly(A) tails and 5' end caps.<sup>10</sup> circRNAs regulate gene expression at the transcriptional or post-transcriptional level by acting as miRNA sponges (competing endogenous RNAs, ceRNAs) or binding to other molecules.<sup>11</sup> Accumulating evidence has suggested that circRNAs play an important role in cancer progression.<sup>12</sup> *circLMTK2* expression was reduced in gastric cancer, suggesting that it might be a novel prognostic biomarker and therapeutic target.<sup>13</sup> Two circRNAs (*hsa\_circRNA\_103809* and *hsa\_circRNA\_104700*) have been implicated in CRC development and as potential biomarkers.<sup>14</sup> RNA sequencing and *in vitro* experiments showed that *circDDX17* was decreased in CRC tissues and might act as a tumor suppressor and novel biomarker.<sup>15</sup> However, previous studies were limited to

Received 27 May 2019; accepted 23 January 2020;  
<https://doi.org/10.1016/j.omtn.2020.01.031>.

<sup>5</sup>These authors contributed equally to this work.

**Correspondence:** Wenjun Zhou, Institute of Digestive Diseases, Longhua Hospital, China-Canada Center of Research for Digestive Diseases (ccCRDD), Shanghai University of Traditional Chinese Medicine, Shanghai 200032, China.  
E-mail: [wjzhou678@163.com](mailto:wjzhou678@163.com)

**Correspondence:** Guang Ji, Institute of Digestive Diseases, Longhua Hospital, China-Canada Center of Research for Digestive Diseases (ccCRDD), Shanghai University of Traditional Chinese Medicine, Shanghai 200032, China.  
E-mail: [jiliver@vip.sina.com](mailto:jiliver@vip.sina.com)



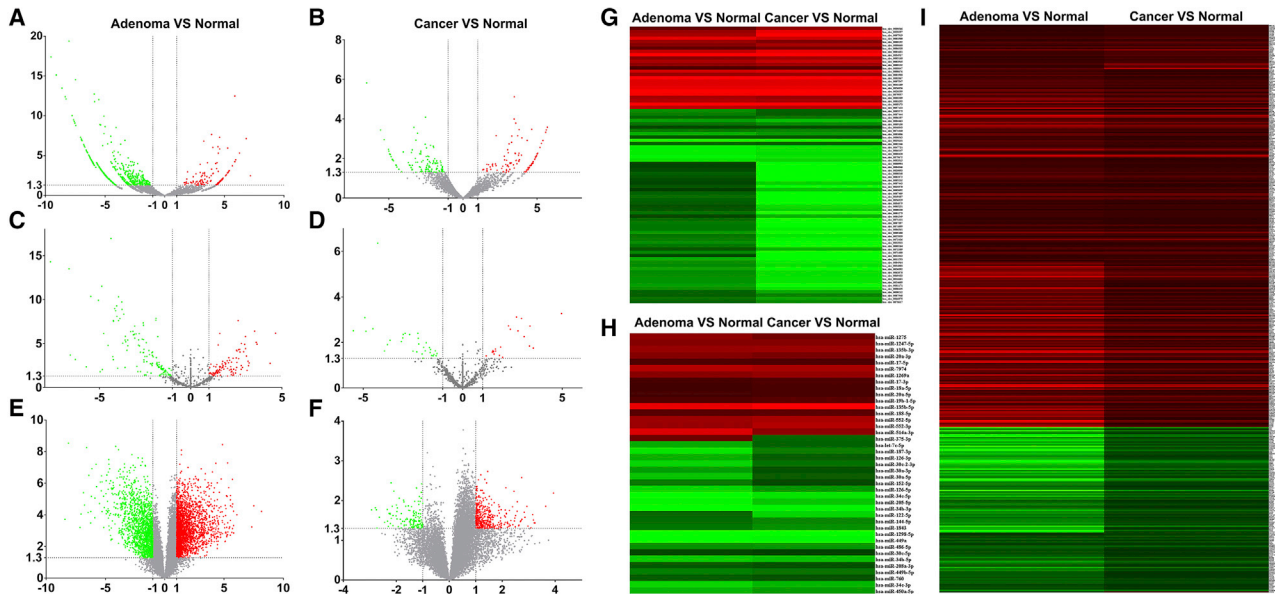


**Figure 1. Identification and Hierarchical Cluster Analysis of Candidate RNAs**

Significantly changed RNAs were visualized in volcano plots. Red and green dots indicate upregulated and downregulated genes, respectively. RNA expression patterns were visualized by hierarchical cluster heatmap. Colors indicate expression values, with brighter red indicating higher values and brighter green lower values. (A and B) Differentially expressed circRNAs in adenoma compared with normal tissues (A) and in CRC compared with normal tissues (B). (C and D) Differentially expressed miRNAs in adenoma compared with normal tissues (C) and in CRC compared with normal tissues (D). (E and F) Differentially expressed mRNAs in adenoma compared with normal tissues (E) and in CRC compared with normal tissues (F). (G–I) Heatmaps of overlapped circRNAs (G), miRNAs (H), and mRNAs (I).

circRNAs that were differentially expressed between CRC and normal tissues, and their expression changes in adenomas were not clarified. Little is therefore known about circRNA-related ceRNAs predicting the adenoma to cancer transition.

We aimed to clarify the pathogenesis of CRC and identify potential biomarkers along the colorectal adenoma to CRC transition by comprehensive expression profiling of circRNAs, miRNAs, and mRNAs in colorectal adenoma, CRC, and adjacent normal tissues. We focused on mining common molecular events in colorectal adenoma and CRC, constructed circRNA-related ceRNA networks, and identified predictive biomarkers and potential therapeutic targets of CRC. Our findings may provide novel perspectives in CRC pathogenesis and suggest possible candidate biomarkers for the early diagnosis and treatment of CRC.

## RESULTS

### Expression profiles of Candidate circRNAs, miRNAs, and mRNAs

A total of 575 differentially expressed circRNAs (DECs), 243 differentially expressed miRNAs (DEMs), and 3,950 differentially expressed mRNAs (DEGs) were identified in colorectal adenoma compared with adjacent normal tissues (adenoma versus normal), and 171 DECs, 53 DEMs, and 506 DEMs in CRC compared with normal tissues (cancer versus normal) (Figures 1A–1F). The overlapped DECs (84), DEMs (41), and DEGs (398) between adenoma versus normal

and cancer versus normal were filtered out using Venn diagrams (see Figure S1). The log-transformed fold changes and p values of representative overlapped DECs, DEMs, and DEGs are listed in Table 1, and the details are described in Tables S1–S3, respectively.

We explored the expression patterns of the overlapped RNAs among the groups by hierarchical cluster analysis. Most of the overlapped RNAs exhibited similar expression patterns in adenoma and CRC tissues compared with adjacent normal tissues (Figures 1G–1I). For example, has-miR-135b-5p, has-miR-20a-5p, and has-miR-17-5p levels were elevated in both adenoma and CRC tissues, whereas hsa\_circ\_0066875, hsa\_circ\_0007444, hsa\_circ\_0049487, *TNSI*, and *SDK1* levels were decreased in both adenoma and CRC samples.

### Functional Enrichment and Protein-Protein Interaction (PPI)

#### Analysis

GO and KEGG pathway enrichment analyses were performed to explore the main biological functions of the overlapped DEGs. Among the top 30 enriched GO terms and KEGG pathways (Figure 2; Tables S4 and S5), regulation of gene silencing, DNA damage checkpoint, cell cycle, p53 signaling pathway, etc. were related to tumorigenesis.

PPI analysis was performed to identify important hub genes among the overlapped DEGs, and a network with 301 nodes was generated

**Table 1. Representative Overlapped RNAs between Adenoma and CRC**

RNA Name	Adenoma versus Normal log <sub>2</sub> (Fold Change)	Adenoma versus Normal p Value	Cancer versus Normal log <sub>2</sub> (Fold Change)	Cancer versus Normal p Value
hsa_circ_0003915	3.93	0.00	3.46	0.00
hsa_circ_0008309	3.06	0.00	3.28	0.00
hsa_circ_0000660	3.34	0.00	2.68	0.02
hsa_circ_0000566	2.97	0.00	2.00	0.02
hsa_circ_0071411	-5.17	0.00	-2.13	0.04
hsa_circ_0049487	-6.75	0.00	-2.19	0.00
hsa_circ_0009130	-2.72	0.03	-2.30	0.02
hsa_circ_0001279	-5.46	0.00	-2.30	0.03
hsa_circ_0066875	-3.26	0.00	-2.30	0.01
hsa_circ_0007444	-1.90	0.00	-2.53	0.00
hsa-miR-449a	-4.96	0.02	-4.92	0.00
hsa-miR-187-3p	-4.53	0.00	-2.50	0.02
hsa-miR-126-5p	-4.27	0.00	-2.99	0.00
hsa-miR-126-3p	-3.49	0.00	-1.88	0.02
hsa-miR-449b-5p	-2.53	0.04	-2.30	0.03
hsa-miR-20a-5p	1.36	0.02	1.49	0.03
hsa-miR-17-3p	1.45	0.02	1.58	0.03
hsa-miR-17-5p	1.63	0.00	1.56	0.02
hsa-miR-135b-3p	3.01	0.00	3.09	0.01
hsa-miR-135b-5p	4.65	0.00	4.97	0.00
<i>CDC6</i>	1.42	0.00	1.37	0.05
<i>CDK1</i>	1.92	0.00	1.58	0.03
<i>DDR2</i>	-4.71	0.00	-1.69	0.03
<i>EFS</i>	-2.48	0.00	-1.15	0.03
<i>FOXN3</i>	-1.42	0.00	-1.23	0.00
<i>IL6R</i>	-1.83	0.00	-1.16	0.05
<i>KLF9</i>	-3.29	0.00	-1.81	0.05
<i>MID2</i>	-1.28	0.00	-1.17	0.04
<i>SDK1</i>	-1.39	0.00	-1.05	0.04
<i>TCF21</i>	-1.48	0.00	-1.16	0.04

(Figure 3A). A total of 180 genes (e.g., *CASP8*, *TNSI*, *CXCL1*, etc.) interacted with more than five other genes. The degree of each node was calculated using CytoNCA, and a sub-network with the top 50 genes (e.g., *CDC6*, *CDK1*, *PTTG1*, etc.) was presented in Figure 3B.

#### miRNA-mRNA Interaction and circRNA-Related ceRNA Network Analysis

To construct circRNA-related ceRNA networks, negatively regulated miRNA-mRNA pairs were first screened and visualized. A network with 24 downregulated miRNAs and 158 upregulated mRNAs was constructed (Figure 4A), e.g., decreased has-126-5p was correlated with two increased mRNAs (*DTL* and *NDC1*). Another network with 17 upregulated miRNAs and 86 downregulated mRNAs was

also generated (Figure 4B), e.g., upregulated hsa-135b-5p interacted with eight downregulated mRNAs (*TNSI*, *SDK1*, and *ALPK3*, etc.). The interaction between miRNAs and circRNAs was predicted using starBase, and a ceRNA network (Figure 4C) was constructed including three downregulated circRNAs (hsa\_circ\_0049487, hsa\_circ\_0066875, and hsa\_circ\_0007444), three upregulated miRNAs (hsa-miR-135b-5p, hsa-miR-20a-5p, and hsa-miR-17-5p), and 25 downregulated mRNAs (*ALPK3*, *TNSI*, *SDK1*, etc.).

#### The Cancer Genome Atlas (TCGA) Database and Real-Time PCR Validation

To validate our findings, the RNA expression levels in the ceRNA network were compared with the TCGA database and confirmed by real-time PCR. The expression patterns of six downregulated mRNAs and two upregulated miRNAs were consistent with the TCGA data (Figures 5A–5H). Another 10 differentially expressed RNAs (three downregulated circRNAs, one upregulated miRNA, and six downregulated mRNAs) were validated by real-time PCR in both colorectal adenoma and cancer tissues (Figures 5I and 5J). The RNA sequencing and real-time PCR results were in good accordance.

#### Receiver Operating Characteristic (ROC) Curve Analysis

The expression levels of three circRNAs (hsa\_circ\_0049487, hsa\_circ\_0066875, and hsa\_circ\_0007444) in the ceRNA network were confirmed by real-time PCR. Literature retrieval revealed that circRNA-related miRNAs and mRNAs in the ceRNA network might play a role in cancer progression, suggesting potential roles for the above three circRNAs in cancer. Therefore, ROC curve analysis was employed to evaluate the diagnostic values of the candidate circRNAs in colorectal adenoma and CRC. The area under the curve (AUC) of hsa\_circ\_0066875 was 0.806, 0.907 in cancer and adenoma, respectively (Figure 6A). The AUC of hsa\_circ\_0007444 was 0.771, 0.682 in cancer and adenoma, respectively (Figure 6B). The AUC of hsa\_circ\_0049487 was 0.809, 1 in cancer and adenoma, respectively (Figure 6C). These results suggested that the above three circRNAs possessed good diagnostic values in colorectal adenoma and cancer and might thus serve as early biomarkers to predict CRC.

#### DISCUSSION

The pathogenesis of CRC is complicated, and an adenoma-carcinoma sequence hypothesis has been proposed. The duration of the adenoma-to-carcinoma transition offers an opportunity to reduce the incidence and mortality of CRC if specific biomarkers can be employed to predict this transition. Identification of specific molecular signatures is urgently needed, and little is currently known about circRNA-related signatures.

In the present study, we employed comprehensive RNA sequencing to obtain circRNA, miRNA, and mRNA expression profiles for adjacent normal, colorectal adenoma, and CRC tissues. We identified several candidates by focusing on the RNAs that are commonly changed in colorectal adenoma and CRC. Integrated analysis of functional enrichment and PPI obtained a batch of hub genes (e.g., *CDC6*, *CDK1*, *PTTG1*, etc.) related to cancer progression. Cell division cycle 6

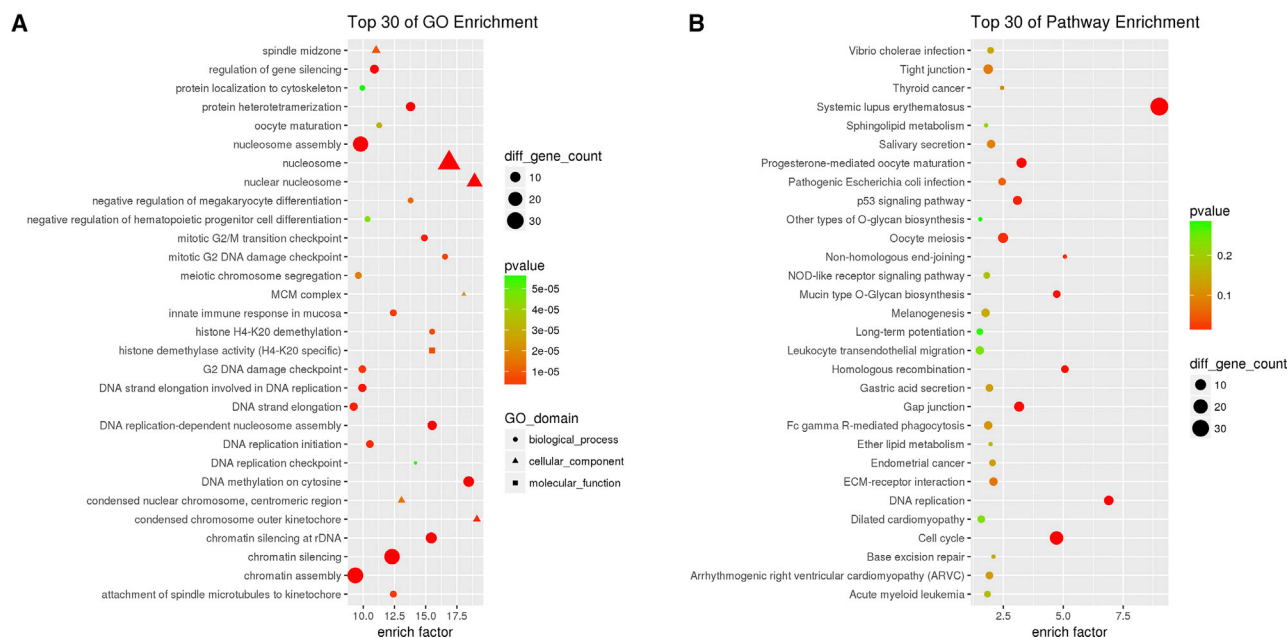


**Figure 2. Functional Enrichment of Candidate DEGs**

(A) Top 30 enriched GO terms; y axis represents GO terms, and x axis represents rich factor. Size and color of the bubble represent number of DEGs enriched in GO terms and enrichment significance, respectively. (B) Top 30 enriched KEGG pathways; y axis represents pathway names, and x axis represents rich factor. Size and color of the bubble represent number of DEGs enriched in the pathway and enrichment significance, respectively.

(CDC6) is an important regulator of cell cycle, and its aberrant expression in human cells poses a serious risk of carcinogenesis.<sup>16</sup> CDC6 has been reported as a potential prognostic marker of lung adenocarcinoma and prostate cancer.<sup>17,18</sup> In the present study, CDC6 expression levels were elevated in both colorectal adenoma and CRC tissues, implying a potential role in the adenoma-to-carcinoma transition. Cyclin-dependent kinase1 (CDK1) is a member of the CDK family associated with cancer development.<sup>19</sup> Previous bioinformatics data mining identified CDK1 as an important hub gene with elevated expression in all CRC stages compared with adjacent normal cells.<sup>20</sup> Our findings were partly consistent with the above previous studies. We noted that the hub gene CDK1 was up-regulated in both human colorectal adenoma and CRC compared with adjacent normal tissues. Pituitary tumor transforming gene-1 (PTTG1) was also overexpressed in colorectal carcinoma tissues and may serve as an oncogene in CRC.<sup>21</sup> In the current study, PTTG1 expression was elevated in both colorectal adenoma and CRC tissues. Further investigation of the hub genes in the present study may obtain novel predictive biomarkers and therapeutic targets to treat CRC.

Long noncoding RNA (lncRNA)-related ceRNA networks have been extensively investigated in human cancers such as hepatocellular carcinoma, breast cancer, as well as CRC.<sup>22–24</sup> However, the involvement of circRNA-related ceRNA networks in CRC, especially their effects in colorectal adenoma and its transition to CRC, remains unclear. In the present study, we constructed three circRNA-related ceRNA

networks using candidate RNAs that overlapped between adenoma and CRC. We noted that two circRNAs (hsa\_circ\_0007444 and hsa\_circ\_0066875) might be ceRNAs of eight mRNAs (*ADCY5*, *ALPK3*, *SDK1*, *MID2*, *TNS1*, *RBPMS*, *GNAZ*, and *RRAS*) by binding to hsa-miR-135b-5p. Although little is known about the biological functions of the above two circRNAs, their related miRNAs and mRNAs have revealed potential roles in cancer. For example, hsa-miR-135b-5p might modulate the *APC* gene and influence gastric carcinogenesis,<sup>25</sup> while *ADCY5* has been associated with several human carcinomas, including breast cancer, prostate cancer, and CRC.<sup>26,27</sup> Regarding the *ALPK3* gene, an analysis of Gene Expression Omnibus (GEO) datasets indicated its relationship with the metastasis of osteosarcoma, which was the most common primary solid bone malignancy.<sup>28</sup> The role of *TNS1* in different types of cancer is controversial. *TNS1* was downregulated in human kidney cancer<sup>29</sup> and breast cancer<sup>30</sup> but upregulated in CRC.<sup>31</sup> We noted that *TNS1* was downregulated in both colorectal adenoma and CRC tissues in the current study. However, further large-scale investigations are needed to confirm the role of *TNS1* in CRC progression. The *RBPMS* gene has been implicated in the migration, invasion, and apoptosis of human CRC cells,<sup>32</sup> and the remaining four genes, *MID2*, *SDK1*, *GNAZ*, and *RRAS*, have also been associated with various human cancers.<sup>33–36</sup>

In addition, we observed that hsa\_circ\_00049487 might be a ceRNA of 18 mRNAs (*ALPK3*, *FOXN3*, *TCF21*, etc.) by sponging two miRNAs (hsa-miR-17-5p and hsa-miR-20a-5p). The biological functions of hsa\_circ\_00049487 have not yet been determined but may be

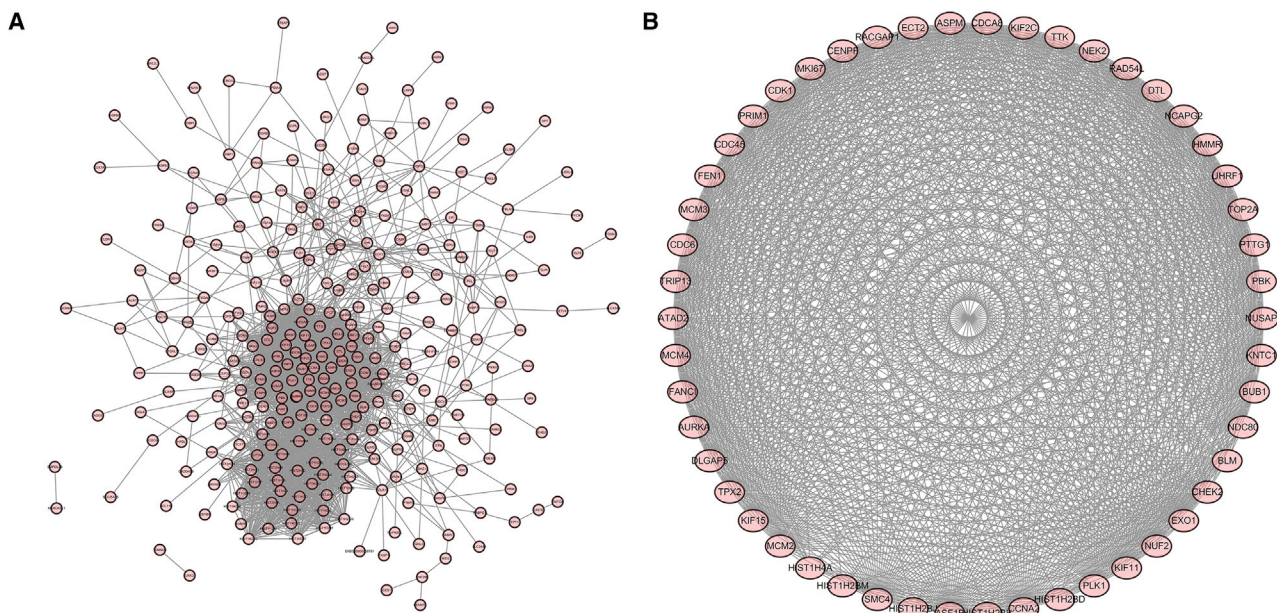


**Figure 3. PPI Networks of Candidate DEGs**

Nodes and edges represent genes and interactions, respectively. (A) PPI network with 301 nodes. (B) Sub-network with top 50 hub genes.

inferred from the related miRNAs and mRNAs. A large-scale pan-cancer analysis identified hsa-miR-17-5p as an oncogenic miRNA,<sup>37</sup> and another study reported that hsa-miR-17-5p and hsa-miR-20a-5p were elevated in human CRC tissues, which might serve as important discriminators for CRC.<sup>38</sup> In the present study, the expression levels of hsa-miR-17-5p and hsa-miR-20a-5p were upregulated in both colorectal adenoma and CRC tissues, which were partly consistent with these previous data. Of interest, the binding targets of the above two miRNAs have been demonstrated in cancer progression. For instance, *FOXN3* was downregulated in colon cancer tissues, and its loss of function promoted colon cancer cell growth, invasion, and

metastasis, indicating its suppressive role in colon cancer.<sup>39</sup> *TCF21* is also a tumor suppressor gene in both human CRC tissues and cells, and its downregulation indicated a poor prognosis in CRC patients.<sup>40,41</sup> We consistently found that *FOXN3* and *TCF21* expression levels were reduced in both colorectal adenoma and CRC tissues.

Overall, our findings suggested that hsa\_circ\_0007444, hsa\_circ\_0066875, and hsa\_circ\_00049487 might play roles in both colorectal adenoma and CRC. Finally, ROC curve analysis revealed that the above three circRNAs could be used to discriminate colorectal adenoma/CRC from adjacent normal tissues and might thus act as early

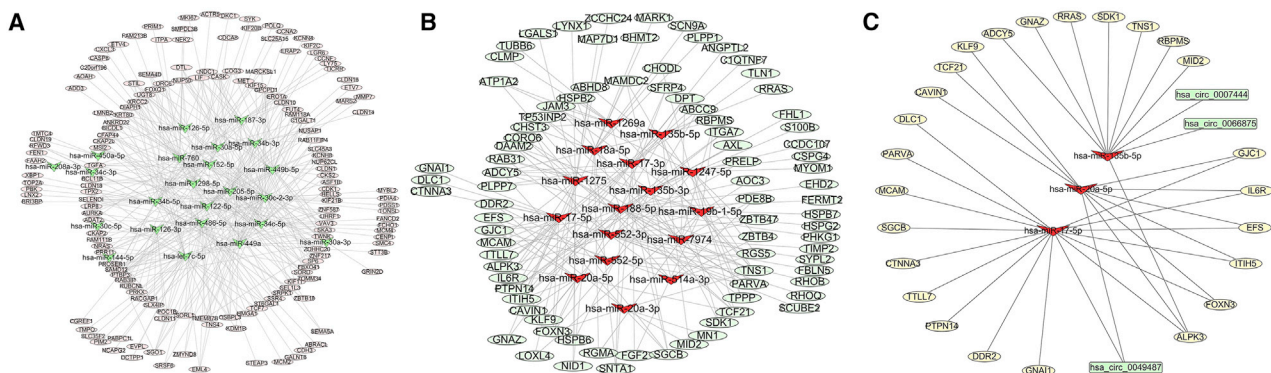


**Figure 4. miRNA-mRNA Regulatory Networks and circRNA-Related ceRNA Network**

Rectangles represent circRNAs, triangles represent miRNAs, ellipses represent mRNAs. Red nodes represent upregulated and green nodes represent downregulated. (A) Downregulated miRNA with upregulated mRNA regulatory network. (B) Upregulated miRNA with downregulated mRNA regulatory network. (C) circRNA-related ceRNA network.

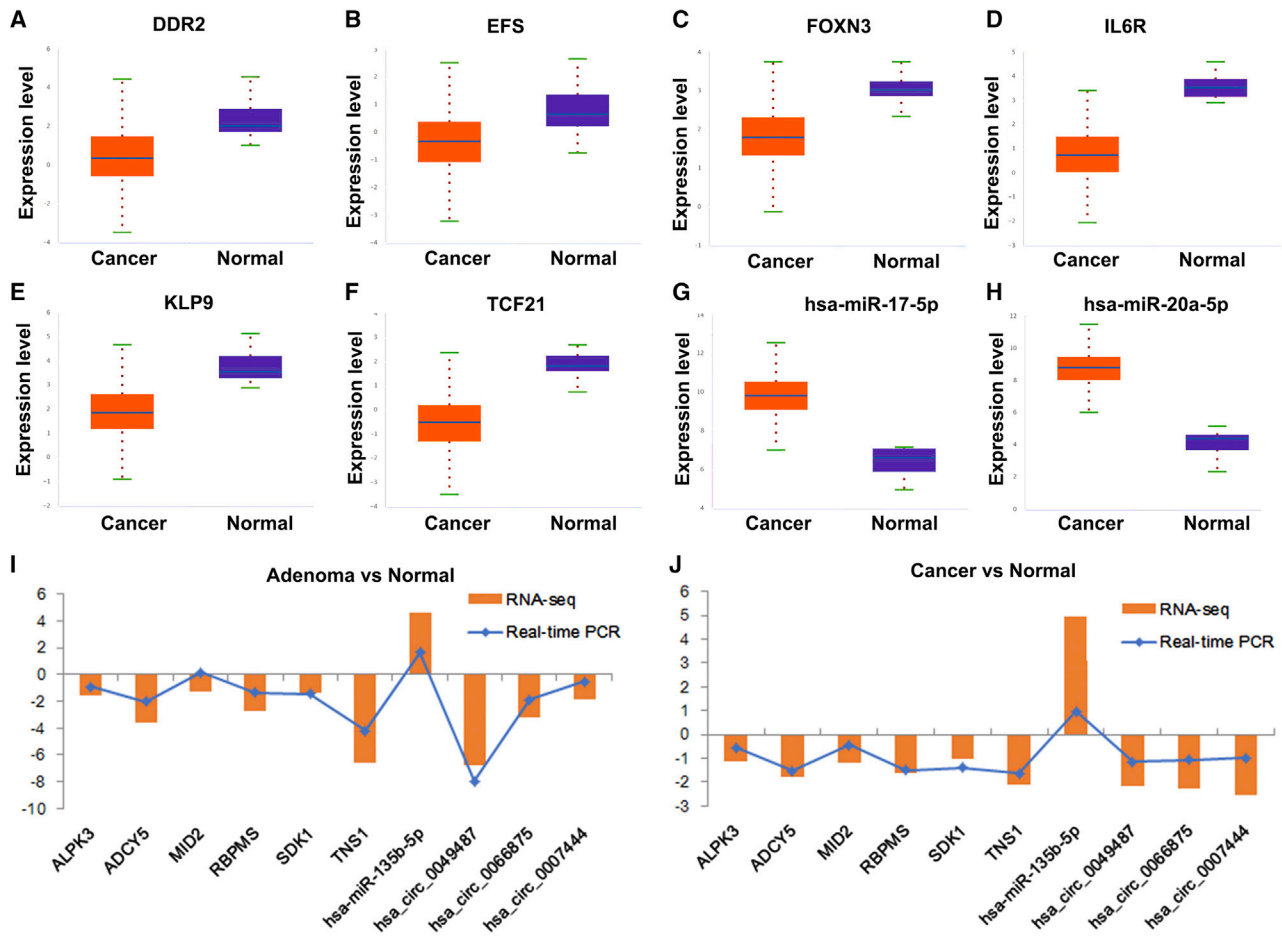


**Figure 5. Representative RNAs Expression Validation**

(A–H) RNA expression levels in cancer and normal samples according to TCGA database, (A) *DDR2*, (B) *EFS*, (C) *FOXN3*, (D) *IL6R*, (E) *KLP9*, (F) *TCF21*, (G) *hsa-miR-17-5p*, (H) *hsa-miR-20a-5p*. (I and J) Real-time PCR validation. The x axis represents RNA names, and the y axis represents  $\log_2$  (fold change) based on the ratio of adenoma and normal average expression values (I) or the ratio of CRC and normal average expression values (J). Brown bars represent real-time PCR data, and blue points represent RNA sequencing data.

predictive biomarkers to prevent CRC. Although novel circRNAs have been strongly associated with the transition from colorectal adenoma to cancer, further studies would be worthy to be investigated. First, our data were based on RNA sequencing expression profiles, and the underlying functions and mechanisms of the circRNA-related ceRNAs are to be clarified. Second, the numbers of clinical samples were limited in the present study, and larger-scale validation is needed to verify these findings.

In conclusion, we comprehensively analyzed the expression profiles of circRNAs, miRNAs, and mRNAs from colorectal adenoma, CRC, and adjacent normal tissues. We mined RNAs that are commonly changed in colorectal adenoma and CRC, constructed circRNA-related ceRNA networks, and identified three novel circRNAs as potential predictive biomarkers and possible therapeutic targets of CRC. Our findings may offer new perspectives for understanding the pathogenesis of the transition from colorectal adenoma

to CRC and provide novel biomarkers and candidate targets for the early diagnosis and treatment of CRC.

## MATERIALS AND METHODS

### Participants and Samples

A total of 90 samples were collected (30 colorectal adenoma, 30 CRC tissues, and 30 adjacent normal tissues) from patients who underwent surgical treatment in Longhua Hospital, Shanghai, China. All resected specimens were snap frozen in liquid nitrogen and stored at  $-80^\circ\text{C}$ . This study was approved by the Ethics Committee of Longhua Hospital, and informed consent was obtained from all participants.

### RNA Extraction and RNA Sequencing Data Acquisition and Processing

Total RNA was extracted from five colorectal adenoma, five CRC, and five adjacent normal tissues using TRIzol reagent (Life Technologies,

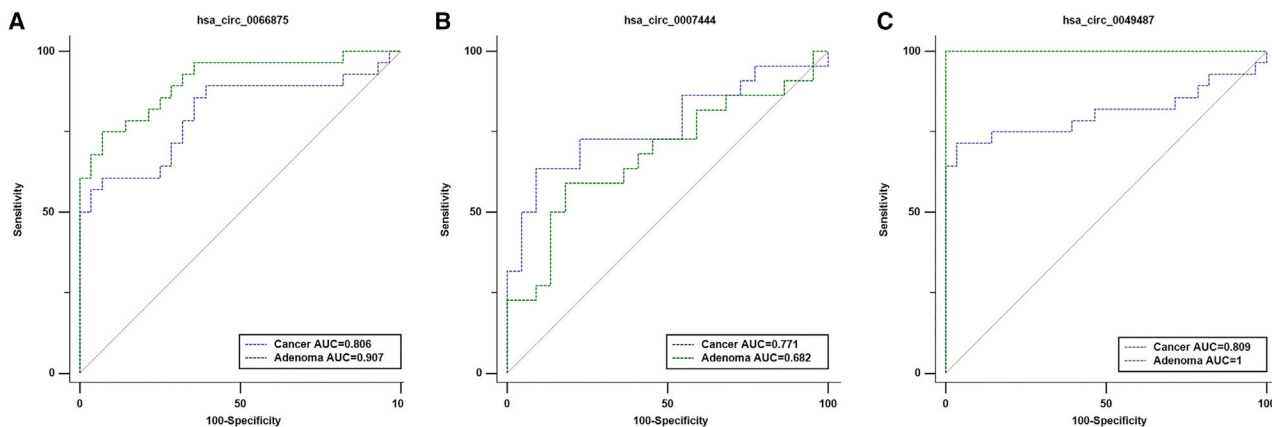


**Figure 6. ROC Curve Analysis of Three circRNAs**

Blue dotted lines represent diagnostic values for discriminating cancer from normal tissues; green dotted lines represent diagnostic values for discriminating adenoma from normal tissues. (A–C) hsa\_circ\_0066875 (A), hsa\_circ\_0007444 (B), and hsa\_circ\_0049487 (C).

CA, USA) following the manufacturer's instructions. The RNA quality was assessed by spectrophotometry and denaturing agarose gel electrophoresis. The RNA sequencing data were acquired as described previously.<sup>42</sup> In brief, the sequencing libraries for circRNAs, miRNAs, and mRNAs were prepared, purified, qualified and sequenced using Illumina HiSeq 4000. Clean reads were obtained and aligned to the human genome. Significantly differentially expressed RNAs were identified using DESeq2 software with a threshold of 2-fold change and p value less than 0.05.

DECs, DEMs, and DEGs were filtered out in pairwise groups (colorectal adenoma versus adjacent normal and CRC versus adjacent normal). The differentially expressed RNAs were visualized on volcano plots constructed by plotting  $-\log_{10}$  (p value) on the y axis and  $\log_2$  (fold change) on the x axis. Overlapped differentially expressed RNAs between colorectal adenoma and CRC tissues (compared with adjacent normal tissues) were obtained by Venn diagrams and subjected to further analysis. Hierarchical cluster analysis was performed to exhibit the expression patterns in pairwise groups.

#### Functional Enrichment and PPI Analysis

We further explored the main biological functions of the identified DEGs by functional enrichment analysis based on the GO and KEGG databases.<sup>43,44</sup> PPI networks were screened based on the String database and visualized using Cytoscape software (version 7.0). The Cytoscape plug-in app CytoNCA was used to calculate the node degree, and the top 50 representative hub nodes with higher degree were filtered out.

#### miRNA-mRNA Interaction and circRNA-Related ceRNA Network Construction

miRNA-mRNA interaction networks were constructed as described previously.<sup>45</sup> To construct the circRNA-related ceRNA networks, interactions between circRNAs and miRNAs were predicted using star-

Base.<sup>46</sup> According to the ceRNA hypothesis, circRNAs act as miRNA sponges and negatively regulate miRNA-mediated gene silencing.<sup>47</sup> Negatively interacting circRNA-miRNA pairs were filtered out, and circRNA-related ceRNA networks were constructed and visualized using Cytoscape software (version 7.0).

#### RNA Expression Validation by TCGA Database and Real-Time PCR

We validated our findings by examining the expression levels of eight RNAs in ceRNA networks by large-scale TCGA data (471 CRC and 41 normal tissues) using the online tool starBase<sup>46</sup> and validated a further 10 RNAs by real-time PCR as described previously.<sup>48</sup> The primer sequences are listed in Table 2.

#### Statistical Analysis

Statistical analysis was performed using MedCalc statistical software (version 15.8). p values less than 0.05 was considered statistically significant. ROC curves were generated, and the AUC was calculated to assess the diagnostic values of circRNA expression for discriminating colorectal adenoma/CRC from normal tissues.

#### SUPPLEMENTAL INFORMATION

Supplemental Information can be found online at <https://doi.org/10.1016/j.omtn.2020.01.031>.

#### AUTHOR CONTRIBUTIONS

G.J. and W.Z. conceived, designed, and supervised the study. M.Z., Y.D., Z.Y., Y.L., L.Z., and Y.X. collected samples. M.Z. and Y.D. performed the experiments and analyzed the data. M.Z., W.Z., and G.J. wrote the paper. All authors reviewed and approved the final manuscript.

#### CONFLICTS OF INTEREST

The authors declare no competing interests.

**Table 2. Primer Sequences in Real-Time PCR Experiments**

RNAs	Primer (5' to 3')
hsa_circ_0049487	forward, CATACACAGGTGCAGTCC
	reverse, GGCTTACCCCATACTTG
hsa_circ_0066875	forward, AGGAGCTGTCACGGGAAGT
	reverse, GAATGAAGCCTCGTGTGG
hsa_circ_0007444	forward, AAGTTGAAAGATTCTGGGGATG
	reverse, TGTGACGCTTCAGCCTTT
hsa-miR-17-5p	forward, CAAAGTGCTTACAGTGCAGGTAG
	reverse, ATCCAGTGCAGGGTCCGAGG
hsa-miR-20a-5p	forward, TAAAGTGCTTATAGTGCAGGTAG
	reverse, ATCCAGTGCAGGGTCCGAGG
hsa-miR-135b-5p	forward, TATGGCTTTTCATTCTATGTGA
	reverse, ATCCAGTGCAGGGTCCGAGG
U6	forward, AGAGAAGATTAGCATGGCCCTG
	reverse, ATCCAGTGCAGGGTCCGAGG
MID2	forward, CCATGACCACCTCCCAAT
	reverse, AAACAACAGCCAACCCCT
TNS1	forward, TGGAGAAGTCGGGCAGAG
	reverse, AGAAGCGAAGGATGTCAGTG
RBPMS	forward, CGGAGTCCAGGGTAAATTAGTAGCA
	reverse, CCAGTTGTGAATAAGCCATAGGTAGAAG
ALPK3	forward, TGAGGCAGAAGTCGGTGG
	reverse, GATTCGGGTGGAGCAGTT
ADCY5	forward, ATCGCCCAGGCTGTAGTT
	reverse, AAGATCGTGCAGTCCAAG
SDK1	forward, ACGATCAGGCTGGACAGAG
	reverse, GTGAATGAGGCGGGCTAC
ACTB	forward, GAAGAGCTACGAGCTGCCTGA
	reverse, CAGACAGCACTGTGTTGGCG

## ACKNOWLEDGMENTS

This work was supported by the National Natural Science Foundation of China (81620108030) and the Key Project of Shanghai 3-year plan (ZY(2018-2020)CCCX-2002-01).

## REFERENCES

- Matyja, M., Pasternak, A., Szura, M., Wysocki, M., Pędziwiatr, M., and Rembiesz, K. (2019). How to improve the adenoma detection rate in colorectal cancer screening? Clinical factors and technological advancements. *Arch. Med. Sci.* *15*, 424–433.
- Zheng, Z.X., Zheng, R.S., Zhang, S.W., and Chen, W.Q. (2014). Colorectal cancer incidence and mortality in China, 2010. *Asian Pac. J. Cancer Prev.* *15*, 8455–8460.
- Laissue, P. (2019). The forkhead-box family of transcription factors: key molecular players in colorectal cancer pathogenesis. *Mol. Cancer* *18*, 5.
- Fearon, E.R., and Vogelstein, B. (1990). A genetic model for colorectal tumorigenesis. *Cell* *61*, 759–767.
- Grady, W.M., and Markowitz, S.D. (2015). The molecular pathogenesis of colorectal cancer and its potential application to colorectal cancer screening. *Dig. Dis. Sci.* *60*, 762–772.
- Ohuchi, M., Sakamoto, Y., Tokunaga, R., Kiyozumi, Y., Nakamura, K., Izumi, D., Kosumi, K., Harada, K., Kurashige, J., Iwatsuki, M., et al. (2018). Increased EZH2 expression during the adenoma-carcinoma sequence in colorectal cancer. *Oncol. Lett.* *16*, 5275–5281.
- Li, X., Kong, L., Liao, S., Lu, J., Ma, L., and Long, X. (2017). The expression and significance of feces cyclooxygenase-2 mRNA in colorectal cancer and colorectal adenomas. *Saudi J. Gastroenterol.* *23*, 28–33.
- Kalmár, A., Péterfia, B., Hollósi, P., Galamb, O., Spisák, S., Wichmann, B., Bodor, A., Tóth, K., Patai, Á.V., Valcz, G., et al. (2015). DNA hypermethylation and decreased mRNA expression of MAL, PRIMA1, PTGDR and SFRP1 in colorectal adenoma and cancer. *BMC Cancer* *15*, 736.
- Nagy, Z.B., Wichmann, B., Kalmár, A., Galamb, O., Barták, B.K., Spisák, S., Tulassay, Z., and Molnár, B. (2017). Colorectal adenoma and carcinoma specific miRNA profiles in biopsy and their expression in plasma specimens. *Clin. Epigenetics* *9*, 22.
- Luo, B., Tang, C.M., and Chen, J.S. (2019). circRNA and gastrointestinal cancer. *J. Cell. Biochem.* *120*, 10956–10963.
- Hansen, T.B., Jensen, T.I., Clausen, B.H., Bramsen, J.B., Finsen, B., Damgaard, C.K., and Kjems, J. (2013). Natural RNA circles function as efficient microRNA sponges. *Nature* *495*, 384–388.
- Zhang, H.D., Jiang, L.H., Sun, D.W., Hou, J.C., and Ji, Z.L. (2018). CircRNA: a novel type of biomarker for cancer. *Breast Cancer* *25*, 1–7.
- He, J., Chen, J., Ma, B., Jiang, L., and Zhao, G. (2019). CircLMTK2 acts as a novel tumor suppressor in gastric cancer. *Biosci. Rep.* *39*, BSR20190363.
- Zhang, P., Zuo, Z., Shang, W., Wu, A., Bi, R., Wu, J., Li, S., Sun, X., and Jiang, L. (2017). Identification of differentially expressed circular RNAs in human colorectal cancer. *Tumour Biol.* *39*, 1010428317694546.
- Li, X.N., Wang, Z.J., Ye, C.X., Zhao, B.C., Li, Z.L., and Yang, Y. (2018). RNA sequencing reveals the expression profiles of circRNA and indicates that circDDX17 acts as a tumor suppressor in colorectal cancer. *J. Exp. Clin. Cancer Res.* *37*, 325.
- Borlado, L.R., and Méndez, J. (2008). CDC6: from DNA replication to cell cycle checkpoints and oncogenesis. *Carcinogenesis* *29*, 237–243.
- Li, S., Xuan, Y., Gao, B., Sun, X., Miao, S., Lu, T., Wang, Y., and Jiao, W. (2018). Identification of an eight-gene prognostic signature for lung adenocarcinoma. *Cancer Manag. Res.* *10*, 3383–3392.
- Kim, Y.H., Byun, Y.J., Kim, W.T., Jeong, P., Yan, C., Kang, H.W., Kim, Y.J., Lee, S.C., Moon, S.K., Choi, Y.H., et al. (2018). CDC6 mRNA Expression Is Associated with the Aggressiveness of Prostate Cancer. *J. Korean Med. Sci.* *33*, e303.
- Zhou, Q. (2017). Targeting Cyclin-Dependent Kinases in Ovarian Cancer. *Cancer Invest.* *35*, 367–376.
- Asghari, M., Abazari, M.F., Bokharai, H., Aleagha, M.N., Poortahmasebi, V., Askari, H., Torabinejad, S., Ardalan, A., Negaresh, N., Ataei, A., et al. (2018). Key genes and regulatory networks involved in the initiation, progression and invasion of colorectal cancer. *Future Sci. OA* *4*, FSO278.
- Ren, Q., and Jin, B. (2017). The clinical value and biological function of PTTG1 in colorectal cancer. *Biomed. Pharmacother.* *89*, 108–115.
- Ye, J., Zhang, J., Lv, Y., Wei, J., Shen, X., Huang, J., Wu, S., and Luo, X. (2019). Integrated analysis of a competing endogenous RNA network reveals key long non-coding RNAs as potential prognostic biomarkers for hepatocellular carcinoma. *J. Cell. Biochem.* *120*, 13810–13825.
- Wang, X., Wan, J., Xu, Z., Jiang, S., Ji, L., Liu, Y., Zhai, S., and Cui, R. (2019). Identification of competitive endogenous RNAs network in breast cancer. *Cancer Med.* *8*, 2392–2403.
- Sha, Q.K., Chen, L., Xi, J.Z., and Song, H. (2019). Long non-coding RNA LINC00858 promotes cells proliferation, migration and invasion by acting as a ceRNA of miR-22-3p in colorectal cancer. *Artif. Cells Nanomed. Biotechnol.* *47*, 1057–1066.
- Magalhães, L., Quintana, L.G., Lopes, D.C.F., Vidal, A.F., Pereira, A.L., D'Araujo Pinto, L.C., de Jesus Viana Pinheiro, J., Khayat, A.S., Goulart, L.R., Burbano, R., et al. (2018). APC gene is modulated by hsa-miR-135b-5p in both diffuse and intestinal gastric cancer subtypes. *BMC Cancer* *18*, 1055.
- Machiela, M.J., Lindström, S., Allen, N.E., Haiman, C.A., Albanes, D., Barricarte, A., Berndt, S.I., Bueno-de-Mesquita, H.B., Chanock, S., Gaziano, J.M., et al. (2012).



- Association of type 2 diabetes susceptibility variants with advanced prostate cancer risk in the Breast and Prostate Cancer Cohort Consortium. *Am. J. Epidemiol.* *176*, 1121–1129.
27. Liang, B., Li, C., and Zhao, J. (2016). Identification of key pathways and genes in colorectal cancer using bioinformatics analysis. *Med. Oncol.* *33*, 111.
  28. Dong, S., Huo, H., Mao, Y., Li, X., and Dong, L. (2019). A risk score model for the prediction of osteosarcoma metastasis. *FEBS Open Bio* *9*, 519–526.
  29. Martuszewska, D., Ljungberg, B., Johansson, M., Landberg, G., Oslakovic, C., Dahlbäck, B., and Hafizi, S. (2009). Tensin3 is a negative regulator of cell migration and all four Tensin family members are downregulated in human kidney cancer. *PLoS ONE* *4*, e4350.
  30. Zhan, Y., Liang, X., Li, L., Wang, B., Ding, F., Li, Y., Wang, X., Zhan, Q., and Liu, Z. (2016). MicroRNA-548j functions as a metastasis promoter in human breast cancer by targeting Tensin1. *Mol. Oncol.* *10*, 838–849.
  31. Zhou, H., Zhang, Y., Wu, L., Xie, W., Li, L., Yuan, Y., Chen, Y., Lin, Y., and He, X. (2017). Elevated transgelin/TNS1 expression is a potential biomarker in human colorectal cancer. *Oncotarget* *9*, 1107–1113.
  32. Hou, N., Guo, Z., Zhao, G., Jia, G., Luo, B., Shen, X., and Bai, Y. (2018). Inhibition of microRNA-21-3p suppresses proliferation as well as invasion and induces apoptosis by targeting RNA-binding protein with multiple splicing through Smad4/extracellular signal-regulated protein kinase signalling pathway in human colorectal cancer HCT116 cells. *Clin. Exp. Pharmacol. Physiol.* *45*, 729–741.
  33. Wang, L., Wu, J., Yuan, J., Zhu, X., Wu, H., and Li, M. (2016). Midline2 is overexpressed and a prognostic indicator in human breast cancer and promotes breast cancer cell proliferation in vitro and in vivo. *Front. Med.* *10*, 41–51.
  34. Yao, S., Hu, Q., Kerns, S., Yan, L., Onitilo, A.A., Misleh, J., Young, K., Lei, L., Bautista, J., Mohamed, M., et al. (2019). Impact of chemotherapy for breast cancer on leukocyte DNA methylation landscape and cognitive function: a prospective study. *Clin. Epigenetics* *11*, 45.
  35. Wang, L., Huang, J., Jiang, M., Lin, H., Qi, L., and Diao, H. (2012). Activated PTHLH coupling feedback phosphoinositide to G-protein receptor signal-induced cell adhesion network in human hepatocellular carcinoma by systems-theoretic analysis. *ScientificWorldJournal* *2012*, 428979.
  36. Xu, L., Gao, Y., Chen, Y., Xiao, Y., He, Q., Qiu, H., and Ge, W. (2016). Quantitative proteomics reveals that distant recurrence-associated protein R-Ras and Transgelin predict post-surgical survival in patients with Stage III colorectal cancer. *Oncotarget* *7*, 43868–43893.
  37. Dhawan, A., Scott, J.G., Harris, A.L., and Buffa, F.M. (2018). Pan-cancer characterisation of microRNA across cancer hallmarks reveals microRNA-mediated downregulation of tumour suppressors. *Nat. Commun.* *9*, 5228.
  38. Pellatt, D.F., Stevens, J.R., Wolff, R.K., Mullany, L.E., Herrick, J.S., Samowitz, W., and Slattery, M.L. (2016). Expression Profiles of miRNA Subsets Distinguish Human Colorectal Carcinoma and Normal Colonic Mucosa. *Clin. Transl. Gastroenterol.* *7*, e152.
  39. Dai, Y., Wang, M., Wu, H., Xiao, M., Liu, H., and Zhang, D. (2017). Loss of FOXN3 in colon cancer activates beta-catenin/TCF signaling and promotes the growth and migration of cancer cells. *Oncotarget* *8*, 9783–9793.
  40. Dai, Y., Duan, H., Duan, C., Zhu, H., Zhou, R., Pei, H., and Shen, L. (2017). TCF21 functions as a tumor suppressor in colorectal cancer through inactivation of PI3K/AKT signaling. *OncoTargets Ther.* *10*, 1603–1611.
  41. Dai, Y., Duan, H., Duan, C., Zhou, R., He, Y., Tu, Q., and Shen, L. (2016). Downregulation of TCF21 by hypermethylation induces cell proliferation, migration and invasion in colorectal cancer. *Biochem. Biophys. Res. Commun.* *469*, 430–436.
  42. Zhu, K.P., Zhang, C.L., Ma, X.L., Hu, J.P., Cai, T., and Zhang, L. (2019). Analyzing the Interactions of mRNAs and ncRNAs to Predict Competing Endogenous RNA Networks in Osteosarcoma Chemo-Resistance. *Mol. Ther.* *27*, 518–530.
  43. Kanehisa, M., Sato, Y., Kawashima, M., Furumichi, M., and Tanabe, M. (2016). KEGG as a reference resource for gene and protein annotation. *Nucleic Acids Res.* *44* (D1), D457–D462.
  44. Ashburner, M., Ball, C.A., Blake, J.A., Botstein, D., Butler, H., Cherry, J.M., Davis, A.P., Dolinski, K., Dwight, S.S., Eppig, J.T., et al.; The Gene Ontology Consortium (2000). Gene ontology: tool for the unification of biology. *Nat. Genet.* *25*, 25–29.
  45. Xia, L., Li, D., Lin, C., Ou, S., Li, X., and Pan, S. (2017). Comparative study of joint bioinformatics analysis of underlying potential of 'neurimmiR', miR-212-3P/miR-132-3P, being involved in epilepsy and its emerging role in human cancer. *Oncotarget* *8*, 40668–40682.
  46. Liu, H., Zhang, Q., Lou, Q., Zhang, X., Cui, Y., Wang, P., Yang, F., Wu, F., Wang, J., Fan, T., and Li, S. (2019). Differential Analysis of lncRNA, miRNA and mRNA Expression Profiles and the Prognostic Value of lncRNA in Esophageal Cancer. *Pathol. Oncol. Res.* Published online April 10, 2019. <https://doi.org/10.1007/s12253-019-00655-8>.
  47. Anstee, Q.M., Reeves, H.L., Kotsiliti, E., Govaere, O., and Heikenwalder, M. (2019). From NASH to HCC: current concepts and future challenges. *Nat. Rev. Gastroenterol. Hepatol.* *16*, 411–428.
  48. Sil, R., and Chakraborti, A.S. (2016). Oxidative Inactivation of Liver Mitochondria in High Fructose Diet-Induced Metabolic Syndrome in Rats: Effect of Glycylrrhizin Treatment. *Phytother. Res.* *30*, 1503–1512.